

Supplementary Data

Cosmogenic nuclide age estimate for Laurentide Ice Sheet recession from the terminal moraine, New Jersey, USA, and constraints on latest Pleistocene ice sheet history

Lee B. Corbett^{*1}, Paul R. Bierman¹, Byron D. Stone², Marc W. Caffee^{3,4,5}, and Patrick L. Larsen¹

* Contact Author: Ashley.Corbett@uvm.edu

¹Department of Geology and School of Natural Resources, University of Vermont, Burlington VT 05405

²United States Geological Survey, East Hartford CT 06103

³Center for Accelerator Mass Spectrometry, Lawrence Livermore National Laboratory, Livermore CA 94550

⁴Department of Physics, Purdue University, West Lafayette IN 47907

⁵Department of Earth, Atmospheric, and Planetary Sciences, Purdue University, West Lafayette IN 47907

Contents:

(Appearing in the order in which they are referred to in the text of the manuscript)

Figure S1: Detailed map of the study area

Table S1: Laboratory preparation information and isotopic data for the 1995 AMS analyses.

Table S2: Detail about blanks included in the 2000 AMS analyses.

Figure S2: Detail about blanks included in the 2000 AMS analyses.

Table S3: Sensitivity analysis for background corrections for the 2000 AMS analyses.

Figure S3: Comparisons between the 1995 and 2000 AMS analyses.

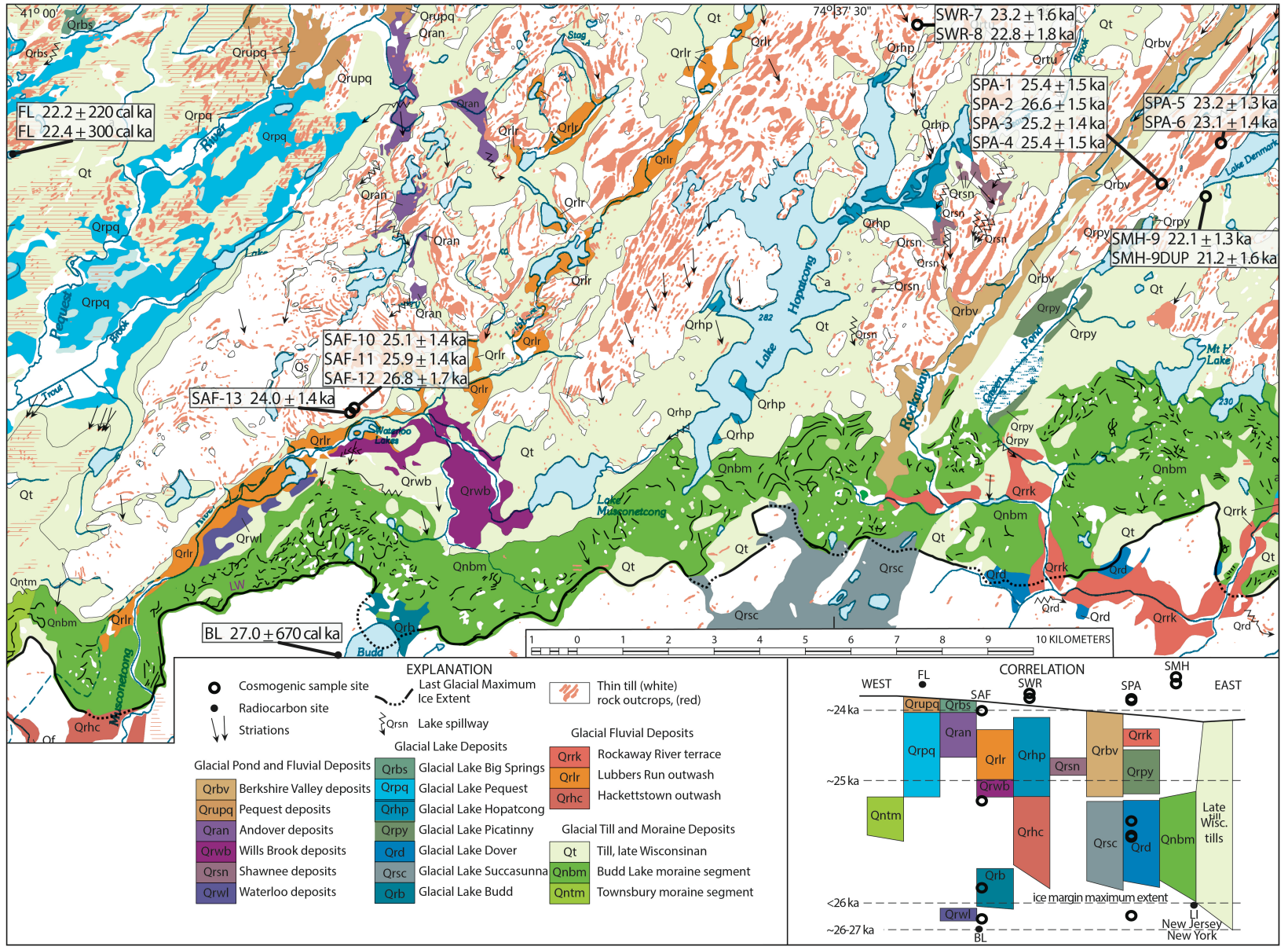


Figure S1 (previous page). Detailed map of the study area (reproduced from Stone et al., 2002), showing late Wisconsinan glacial geology in the terminal moraine area, New Jersey Highlands, and cosmogenic and radiocarbon age constraint. Sample sites show ^{10}Be ages and 1σ external uncertainties. Radiocarbon ages are detailed in Table 1 of the text. The correlation diagram shows relative ages of 19 allostratigraphic units. In addition to till and two moraine segments, units include one glacial-advance sub till deposit (Qrwl), deposits of three moraine-dammed glacial lakes, and one outwash deposit on the distal (south) side of the moraine, all correlated with the Last Glacial Maximum extent during construction of the moraine. To the north, younging units deposited in different basins during ice-margin recession include five units composed of pond and fluvial sediments, deposits of four glacial lakes, and two meltwater fluvial terrace units. Ages of correlated ice-margin positions among the stratigraphic units are based on pre-, syn-, and postglacial dated materials and constraining cosmogenic exposure ages, discussed in text. Sample locations: BL – Budd Lake, FL – Francis Lake, SAF – Allamuchy Forrest, SMH, SPA – Picatinny Arsenal, SWR – Welden Road. Line symbols show crests of narrow ridges in moraine; line of Last Glacial Maximum extent dotted where concealed. Holocene deposits and materials south of terminal moraine are not shown here.

Table S1. Sample preparation information and isotopic data from the original set of sample analyses (from the year 1995) presented in Larsen (1996).

Sample Name	Quartz Mass (g) ^a	⁹ Be Added (μg) ^a	ICP-Quantified Total ²⁷ Al (g) ^a	Be Cathode Number ^a	Be AMS Standard	Al Cathode Number ^a	Al AMS Standard	Measured ¹⁰ Be/ ⁹ Be ^b	¹⁰ Be/ ⁹ Be Uncertainty ^b	¹⁰ Be Concentration (atoms g ⁻¹)	¹⁰ Be Uncertainty (atoms g ⁻¹)	Correction Factor ^c	07KNSTD ¹⁰ Be Concentration (atoms g ⁻¹) ^d	07KNSTD ¹⁰ Be Uncertainty (atoms g ⁻¹) ^d	Measured ²⁶ Al/ ²⁷ Al ^b	²⁶ Al/ ²⁷ Al Uncertainty ^b	²⁶ Al Concentration (atoms g ⁻¹)	²⁶ Al Uncertainty (atoms g ⁻¹)
SAF-10-X	29.877	309	3650	BE4612	LLNL10000	AL1496	KNSTD9900	2.228E-13	1.520E-14	1.522E+05	1.038E+04	0.9042	1.376E+05	9.387E+03	2.950E-13	2.570E-14	8.045E+05	7.009E+04
SAF-11	22.360	249	1900	BE4334	LLNL10000	AL1450	KNSTD9900	1.875E-13	1.290E-14	1.379E+05	9.487E+03	0.9042	1.247E+05	8.578E+03	3.858E-13	2.380E-14	7.318E+05	4.515E+04
SAF-12	28.232	391	3664	BE4216	LLNL10000	AL1350	KNSTD9860	1.457E-13	1.200E-14	1.333E+05	1.098E+04	0.9042	1.205E+05	9.924E+03	2.839E-13	1.900E-14	8.225E+05	5.505E+04
SAF-13-X	25.210	250	2357	BE4341	LLNL10000	AL1449	KNSTD9900	1.819E-13	1.180E-14	1.191E+05	7.728E+03	0.9042	1.077E+05	6.987E+03	4.861E-13	3.450E-14	1.015E+06	7.201E+04
SAF-14	27.680	243	2650	BE4217	LLNL10000	AL1349	KNSTD9860	2.464E-13	2.300E-14	1.429E+05	1.333E+04	0.9042	1.292E+05	1.206E+04	3.858E-13	1.340E-14	8.245E+05	2.864E+04
SMH-9-X	32.694	254	4670	BE4339	LLNL10000	AL1441	KNSTD9900	2.171E-13	1.370E-14	1.114E+05	7.029E+03	0.9042	1.007E+05	6.356E+03	1.584E-13	1.250E-14	5.051E+05	3.986E+04
SPA-1	28.918	311	6521	BE4610	LLNL10000	AL1498	KNSTD9900	2.228E-13	1.520E-14	1.582E+05	1.080E+04	0.9042	1.431E+05	9.761E+03	1.773E-13	1.430E-14	8.925E+05	7.199E+04
SPA-2-X	29.785	270	7065	BE4348	LLNL10000	AL1443	KNSTD9900	2.137E-13	1.300E-14	1.279E+05	7.782E+03	0.9042	1.157E+05	7.037E+03	1.323E-13	1.250E-14	7.006E+05	6.619E+04
SPA-3	24.130	311	5011	BE4615	LLNL10000	AL1449	KNSTD9900	1.860E-13	1.770E-14	1.583E+05	1.507E+04	0.9042	1.431E+05	1.362E+04	1.970E-13	1.710E-14	9.133E+05	7.927E+04
SPA-4-X	27.997	252	6869	BE4726	LLNL10000	AL1639	KNSTD9900	2.597E-13	2.030E-14	1.544E+05	1.207E+04	0.9042	1.396E+05	1.091E+04	1.491E-13	1.430E-14	8.166E+05	7.832E+04
SPA-5-XX	29.030	254	4734	BE4727	LLNL10000	AL1642	KNSTD9900	2.275E-13	1.600E-14	1.315E+05	9.245E+03	0.9042	1.189E+05	8.359E+03	2.486E-13	1.900E-14	9.050E+05	6.917E+04
SPA-6-XX	29.134	259	7993	BE4728	LLNL31000	AL1641	KNSTD9900	2.300E-13	2.390E-14	1.350E+05	1.403E+04	0.8761	1.183E+05	1.229E+04	1.004E-13	1.430E-14	6.149E+05	8.758E+04
SPA-15	28.038	309	6230	BE4613	LLNL10000	AL1500	KNSTD9900	N.D.	N.D.	N.D.	N.D.	N.D.	N.D.	N.D.	1.871E-13	1.610E-15	9.281E+05	7.986E+03
SPA-16-X	34.785	256	8139	BE4729	LLNL10000	AL1643	KNSTD9900	N.D.	N.D.	N.D.	N.D.	N.D.	N.D.	N.D.	1.467E-13	1.250E-14	7.663E+05	6.529E+04
SWR-7	21.786	306	2598	BE4614	LLNL10000	AL1497	KNSTD9900	N.D.	N.D.	N.D.	N.D.	N.D.	N.D.	N.D.	N.D.	N.D.	N.D.	N.D.
SWR-8-X	29.860	252	1759	BE4343	LLNL10000	AL1446	KNSTD9900	2.370E-13	1.330E-14	1.321E+05	7.413E+03	0.9042	1.194E+05	6.702E+03	5.454E-13	3.550E-14	7.172E+05	4.668E+04

^aMasses and cathode numbers are presented in Table 3.3 of Larsen (1996); AMS standard information was provided by R. Finkel.

^bRatio data are presented in Tables 3.4 and 3.5 of Larsen (1996); ratios have been corrected for backgrounds as described in Larsen (1996).

^cCorrection factors for Be data measured against different AMS standards are available at http://hess.ess.washington.edu/math/docs/al_be_v22/AlBe_standardization_table.pdf.

^dConcentrations have been scaled to 07KNSTD (Nishiizumi et al. 2007).

Table S2. Blank data from process blanks included in the three batches of samples for the latter set of analyses (year 2000). Sample ratios calculated with these background values appear in Table 3 of the main text.

Blank Name	$^{10}\text{Be}/^9\text{Be}$ Ratio	$^{10}\text{Be}/^9\text{Be}$ Ratio Unc.	$^{26}\text{Al}/^{27}\text{Al}$ Ratio	$^{26}\text{Al}/^{27}\text{Al}$ Ratio Unc.
164BLK	2.342E-14	1.302E-15	2.449E-15	1.001E-15
164BLKX	1.926E-14	1.003E-15	---	---
165BLK	3.095E-14	2.204E-15	3.205E-15	1.851E-15
165BLKX	2.460E-14	6.211E-15	---	---
166BLK	3.816E-14	2.250E-15	2.155E-15	1.245E-15
166BLKX	3.191E-14	1.856E-15	---	---
AVERAGE	2.805E-14		2.603E-15	
STDEV	6.873E-15		5.414E-16	

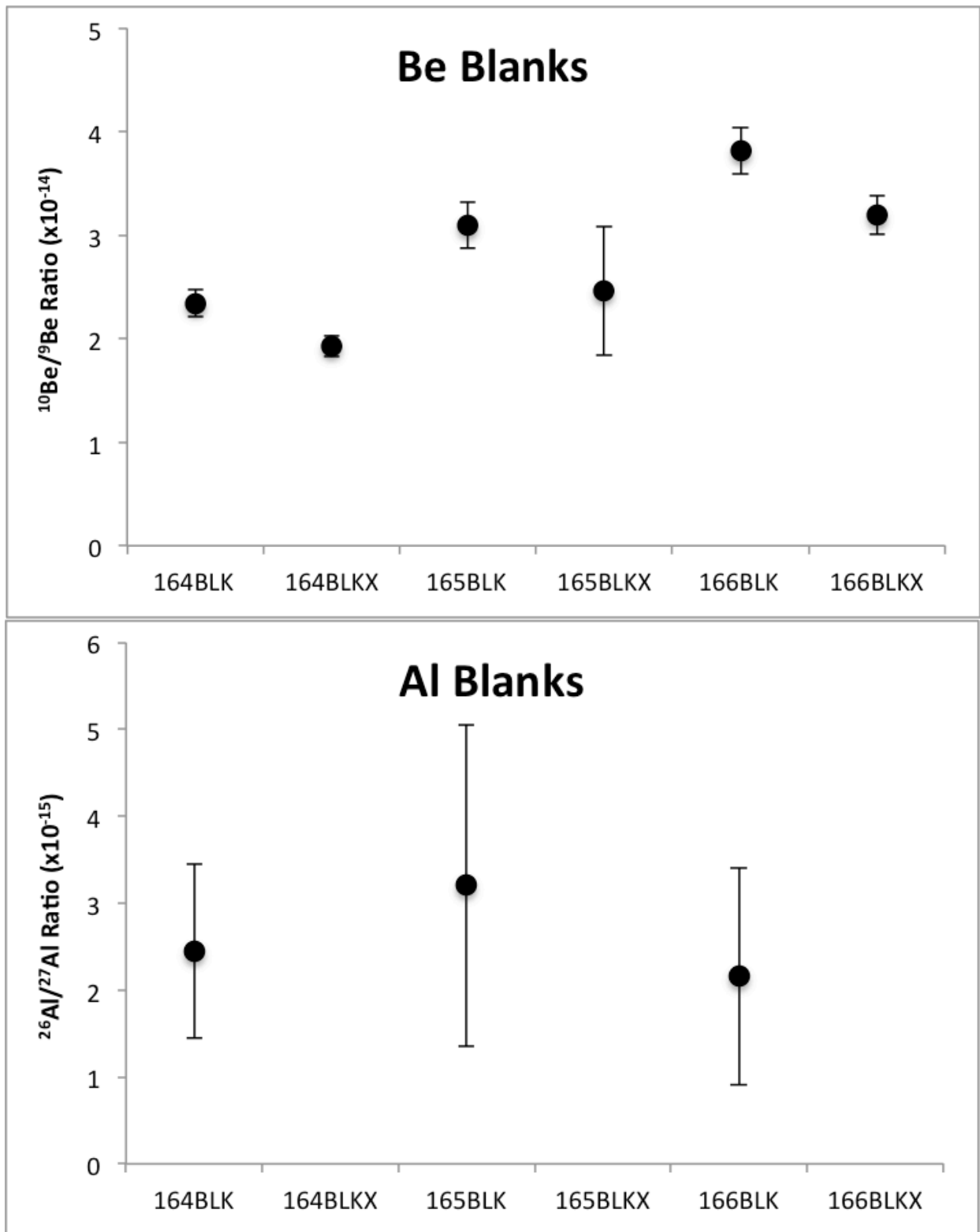


Figure S2. Blank data from process blanks included in the three batches of samples for the latter set of analyses (year 2000). Sample ratios calculated with these background values appear in Table 3 of the main text

Table S3. Sensitivity analysis assessing two different possible background correction schemes (average blank value versus batch-by-batch) and the impact on calculated ^{10}Be and ^{26}Al concentrations for the latter (year 2000) set of analyses. Blank detail is shown in Table S2 and Figure S2.

10Be Data			Sample Name	26Al Data		
Conc. Using Average Blank	Conc. Using Batch-By-Batch Blank	% Difference		Conc. Using Average Blank	Conc. Using Batch-By-Batch Blank	% Difference
1.327E+05	1.353E+05	2.0	SAF-10	8.119E+05	8.122E+05	0.0
1.348E+05	1.376E+05	2.0	SAF-11	7.899E+05	7.901E+05	0.0
1.418E+05	1.420E+05	0.1	SAF-12	9.605E+05	9.591E+05	0.1
1.189E+05	1.191E+05	0.1	SAF-13	7.525E+05	7.517E+05	0.1
1.417E+05	1.419E+05	0.1	SAF-14	8.461E+05	8.450E+05	0.1
1.103E+05	1.132E+05	2.5	SMH-9	6.695E+05	6.699E+05	0.1
1.061E+05	1.062E+05	0.1	SMH-9-DUP	6.916E+05	6.901E+05	0.2
1.384E+05	1.354E+05	2.1	SPA-1	8.307E+05	8.329E+05	0.3
1.408E+05	1.379E+05	2.1	SPA-2	8.643E+05	8.663E+05	0.2
1.375E+05	1.345E+05	2.2	SPA-3	7.818E+05	7.839E+05	0.3
1.367E+05	1.338E+05	2.2	SPA-4	8.176E+05	8.197E+05	0.3
1.222E+05	1.192E+05	2.4	SPA-5	6.989E+05	7.004E+05	0.2
1.334E+05	1.362E+05	2.1	SPA-6	5.605E+05	5.612E+05	0.1
1.227E+05	1.198E+05	2.4	SPA-6-DUP	6.728E+05	6.755E+05	0.4
1.533E+05	1.534E+05	0.1	SPA-15	8.415E+05	8.380E+05	0.4
1.488E+05	1.489E+05	0.1	SPA-16	9.656E+05	9.628E+05	0.3
1.286E+05	1.335E+05	3.8	SWR-7	8.228E+05	8.231E+05	0.0
1.265E+05	1.315E+05	3.9	SWR-8	8.211E+05	8.215E+05	0.0
	AVERAGE:	1.7		AVERAGE:	0.2	
	STDEV:	1.3		STDEV:	0.1	

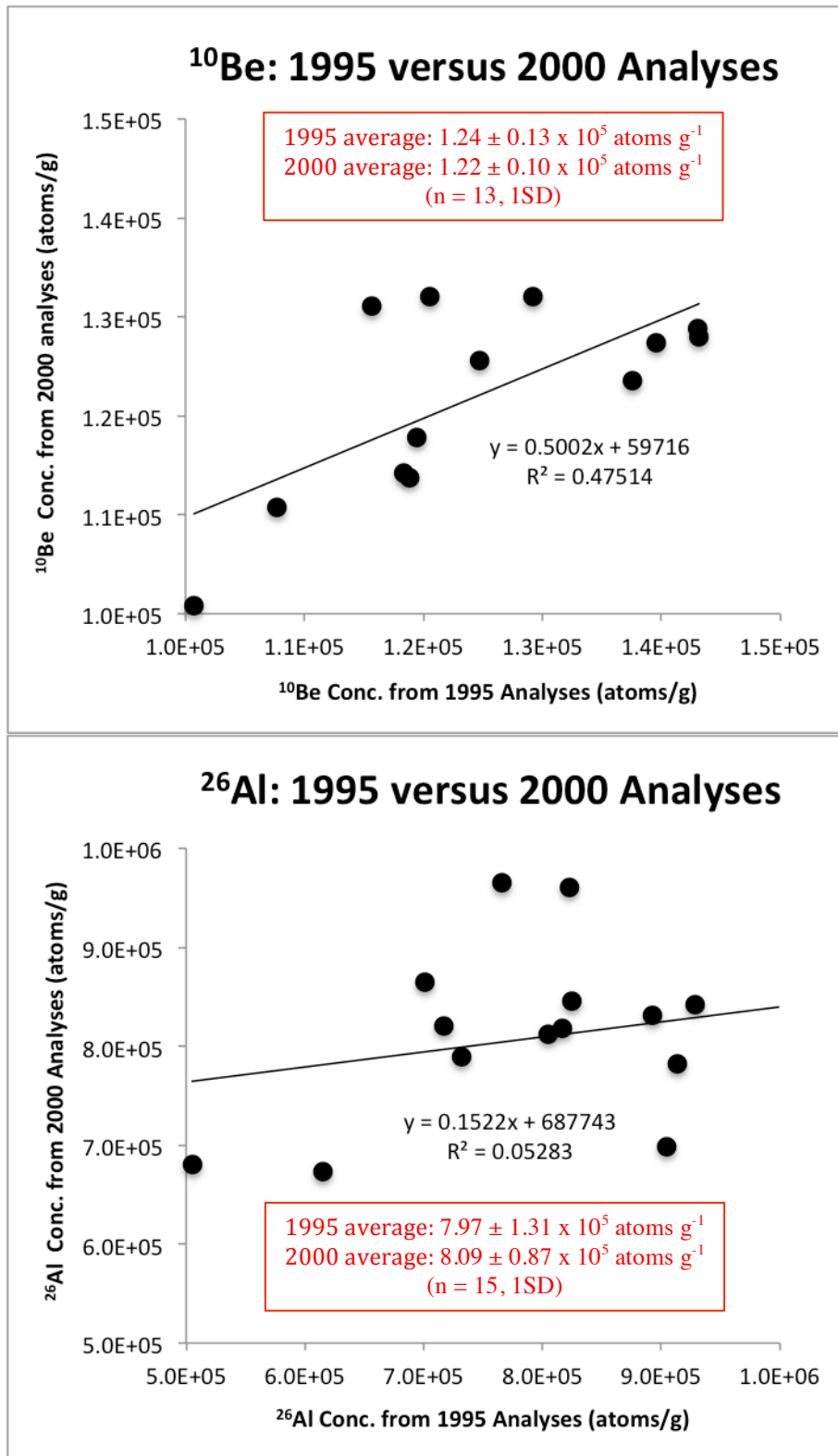


Figure S3. Comparison of isotopic concentrations calculated based on the original set of analyses (from 1995, described in Larsen (1996), Table S1) versus the newer set of analyses (from 2000, the focus of the main text, Table 4).